

Effect of Particle Size on the Kinetics of the Electrocatalytic Oxygen Reduction Reaction Catalyzed by Pt Dendrimer-Encapsulated Nanoparticles

Heechang Ye, John A. Crooks, and Richard M. Crooks*

Department of Chemistry and Biochemistry, Texas Materials Institute, Center for Nano and Molecular Science and Technology, The University of Texas at Austin, 1 University Station, A5300, Austin, Texas 78712-0165

Received July 29, 2007. In Final Form: August 12, 2007

Platinum dendrimer-encapsulated nanoparticles (DENs) containing an average of 55, 100, 147, 200, and 240 atoms were prepared within sixth-generation, hydroxyl-terminated, poly(amidoamine) dendrimers. These DENs were immobilized on glassy carbon electrodes, and the effect of particle size on the kinetics of the oxygen reduction reaction (ORR) was quantitatively evaluated using rotating disk voltammetry. The total areas of the Pt DENs were determined by electrochemical CO stripping and hydrogen desorption, and the results were found to be in reasonable agreement with calculated values. The largest particles exhibited the highest specific activities for the ORR.

Introduction

In this paper, we show that the rate of the Pt-catalyzed electrochemical oxygen reduction reaction (ORR) is a strong function of the catalyst size over the range of 1–2 nm. This is an important finding, because it has heretofore been impossible to quantitatively study ORR kinetics using well-defined Pt particles in this size range due to difficulties associated with their synthesis and characterization.

The catalysts used in this study were Pt dendrimer-encapsulated nanoparticles (DENs). DENs are prepared by a two-step templating procedure.¹ First, suitable dendrimers and metal ions are mixed in a desired stoichiometric ratio. This results in complexation of the metal ions with functional groups within the dendrimers. Second, addition of a reducing agent to these metal ion/dendrimer composites results in conversion of the encapsulated ions to atoms and subsequent agglomeration into particles. Because each dendrimer originally contained nominally the same number of metal ions, this method results in nearly monodisperse particle-size distributions. Moreover, because the dendrimers are porous, much of the encapsulated nanoparticle surface is catalytically active. Finally, the size of encapsulated particles can be controlled via the initial metal ion-to-dendrimer ratio.^{1–4} This dendrimer templating method has been used to synthesize Pt,^{5–9} Pd,^{2,6,10–13} Au,^{3,14–16} Cu,¹⁷ Ni,¹⁸ and Fe¹⁹ monometallic

particles and PtPd,^{9,20,21} PdAu,²² PtAu,²³ and AuAg²⁴ bimetallic (alloy or core–shell) particles.¹ DENs have been used as catalysts for homogeneous hydrogenation and carbon–carbon coupling reactions,^{13,25} as well as for heterogeneous catalytic reactions.^{26,27} Moreover, we recently reported that Pt monometallic and PtPd bimetallic DENs can be immobilized on glassy carbon electrodes and that the resulting DEN films are stable and electrocatalytically active for the ORR.^{8,9} We have also shown that it is possible to measure quantitative electrochemical kinetic rates for the ORR as a function of the composition of bimetallic PtPd DENs.⁹ Finally, Vijayaraghavan and Stevenson have immobilized Pt DENs onto nitrogen-doped carbon nanotubes and demonstrated that such composites catalyze the ORR.²⁸

At the present time, Pt is considered to be the most effective catalyst for the ORR, which is the cathode reaction in hydrogen-based fuel cells. However, Pt is not optimal for this application, because of its high overpotential for the ORR and because it is a scarce element. There are two ways to reduce or eliminate the use of Pt in fuel cells. First, it may be possible to dilute the Pt atoms with a second metal without compromising the electro-

* To whom correspondence should be addressed. Phone: 512-475-8674. Fax: 512-475-8651. E-mail: crooks@cm.utexas.edu.

(1) Scott, R. W. J.; Wilson, O. M.; Crooks, R. M. *J. Phys. Chem. B* **2005**, *109*, 692–704, and references therein.

(2) Wilson, O. M.; Knecht, M. R.; Garcia-Martinez, J. C.; Crooks, R. M. *J. Am. Chem. Soc.* **2006**, *128*, 4510–4511.

(3) Kim, Y.-G.; Oh, S.-K.; Crooks, R. M. *Chem. Mater.* **2004**, *16*, 167–172.

(4) Kim, Y.-G.; Garcia-Martinez, J. C.; Crooks, R. M. *Langmuir* **2005**, *21*, 5485–5491.

(5) Zhao, M.; Crooks, R. M. *Adv. Mater.* **1999**, *11*, 217–220.

(6) Zhao, M.; Crooks, R. M. *Angew. Chem., Int. Ed.* **1999**, *38*, 364–366.

(7) Esumi, K.; Nakamura, R.; Suzuki, A.; Torigoe, K. *Langmuir* **2000**, *16*, 7842–7846.

(8) Ye, H.; Crooks, R. M. *J. Am. Chem. Soc.* **2005**, *127*, 4930–4934.

(9) Ye, H.; Crooks, R. M. *J. Am. Chem. Soc.* **2007**, *129*, 3627–3633.

(10) Scott, R. W. J.; Ye, H.; Henriquez, R. R.; Crooks, R. M. *Chem. Mater.* **2003**, *15*, 3873–3878.

(11) Li, Y.; El-Sayed, M. A. *J. Phys. Chem. B* **2001**, *105*, 8938–8943.

(12) Ooe, M.; Murata, M.; Mizugaki, T.; Ebitani, K.; Kaneda, K. *Nano Lett.* **2002**, *2*, 999–1002.

(13) Garcia-Martinez, J. C.; Lezutekong, R.; Crooks, R. M. *J. Am. Chem. Soc.* **2005**, *127*, 5097–5103.

(14) Gröhn, F.; Bauer, B. J.; Akpalu, Y. A.; Jackson, C. L.; Amis, E. J. *Macromolecules* **2000**, *33*, 6042–6050.

(15) Gröhn, F.; Gu, X.; Gröll, H.; Meredith, J. C.; Nisato, G.; Bauer, B. J.; Karim, A.; Amis, E. J. *Macromolecules* **2002**, *35*, 4852–4854.

(16) Esumi, K.; Satoh, K.; Torigoe, K. *Langmuir* **2001**, *17*, 6860–6864.

(17) Zhao, M.; Sun, L.; Crooks, R. M. *J. Am. Chem. Soc.* **1998**, *120*, 4877–4878.

(18) Knecht, M. R.; Garcia-Martinez, J. C.; Crooks, R. M. *Chem. Mater.* **2006**, *18*, 5039–5044.

(19) Knecht, M. R.; Crooks, R. M. *New J. Chem.* **2007**, *31*, 1349–1353.

(20) Scott, R. W. J.; Datye, A. K.; Crooks, R. M. *J. Am. Chem. Soc.* **2003**, *125*, 3708–3709.

(21) Chung, Y.-M.; Rhee, H.-K. *Catal. Lett.* **2003**, *85*, 159–164.

(22) Scott, R. W. J.; Wilson, O. M.; Oh, S.-K.; Kenik, E. A.; Crooks, R. M. *J. Am. Chem. Soc.* **2004**, *126*, 15583–15591.

(23) Lang, H.; Maldonado, S.; Stevenson, K. J.; Chandler, B. D. *J. Am. Chem. Soc.* **2004**, *126*, 12949–12956.

(24) Wilson, O. M.; Scott, R. W. J.; Garcia-Martinez, J. C.; Crooks, R. M. *J. Am. Chem. Soc.* **2005**, *127*, 1015–1024.

(25) Niu, Y.; Crooks, R. M. *C. R. Chimie* **2003**, *6*, 1049–1059.

(26) Lang, H.; May, R. A.; Iversen, B. L.; Chandler, B. D. *J. Am. Chem. Soc.* **2003**, *125*, 14832–14836.

(27) Scott, R. W. J.; Wilson, O. M.; Crooks, R. M. *Chem. Mater.* **2004**, *16*, 5682–5688.

(28) Vijayaraghavan, G.; Stevenson, K. J. *Langmuir* **2007**, *23*, 5279–5282.

catalytic properties of pure Pt.^{29,30} A limiting case of this approach is to eliminate Pt altogether, using appropriate multimetallic catalysts.^{30–35} Second, it is possible to reduce the particle size so that each atom in the particle is used as efficiently as possible. From a purely geometric perspective, this means using particles that contain minimal subsurface Pt atoms. This paper addresses this latter approach.

For a fixed mass of metal the total number of surface atoms increases as particle size decreases. However, it has been reported that smaller Pt nanoparticles do not necessarily provide better catalytic mass activities for the ORR because of their size-dependent geometric and electronic properties.^{36–42} For example, Kinoshita and co-workers proposed that the decrease in ORR activity could be linked to a reduction in the fraction of desirable crystal faces available for the ORR for particles having diameters of less than ~ 10 nm.³⁸ It has also been proposed that lower ORR kinetics result from strong adsorption of oxygenated species, which are thought to prevent the ORR, to the surface of smaller Pt particles.^{30,39–41} Other reports have suggested altogether different explanations for the effect of catalyst size on the rate of the ORR.^{43–46} For example, Watanabe and co-workers reported that interparticle spacing, rather than particle size, dominate rate measurements for closely spaced catalysts.^{44–46} Indeed, they found that catalysts separated by less than about 20 nm exhibit no particle-size dependence on specific activity. A review of the recent literature in this field makes three clear points. First, there is consensus that there is a strong correlation between Pt particle size and ORR kinetics. Second, the reason for this relationship is not fully understood. Third, studies reported to date have focused on particles having sizes and size distributions larger than those used here, presumably because of the difficulty associated with the synthesis and characterization of particles in the < 2 nm size range.

In this paper, we utilize the dendrimer templating method to prepare 1–2 nm-diameter Pt nanoparticle catalysts having low (± 0.3 nm) size polydispersity. These materials are used to better understand the effect of Pt catalyst size on the activity of the ORR using rotating disk voltammetry. The quantitative kinetic results indicate that the specific activity for the Pt-catalyzed ORR decreases monotonically as the particle size decreases.

(29) Markovic, N. M.; Schmidt, T. J.; Stamenkovic, V.; Ross, P. N. *Fuel Cells* **2001**, *1*, 105–116.

(30) Gasteiger, H. A.; Kocha, S. S.; Sompalli, B.; Wagner, F. T. *Appl. Catal. B: Environ.* **2005**, *56*, 9–35.

(31) Wang, B. J. *Power Sources* **2005**, *152*, 1–15.

(32) Fernández, J. L.; Walsh, D. A.; Bard, A. J. *J. Am. Chem. Soc.* **2005**, *127*, 357–365.

(33) Fernández, J. L.; Raghuvveer, V.; Manthiram, A.; Bard, A. J. *J. Am. Chem. Soc.* **2005**, *127*, 13100–13101.

(34) Raghuvveer, V.; Manthiram, A.; Bard, A. J. *J. Phys. Chem. B* **2005**, *109*, 22909–22912.

(35) Shao, M.-H.; Sasaki, K.; Adzic, R. R. *J. Am. Chem. Soc.* **2006**, *128*, 3526–3527.

(36) Peuckert, M.; Yoneda, T.; Dalla Betta, R. A.; Boudart, M. *J. Electrochem. Soc.* **1986**, *133*, 944–947.

(37) Sattler, M. L.; Ross, P. N. *Ultramicroscopy* **1986**, *20*, 21–28.

(38) Kinoshita, K. *J. Electrochem. Soc.* **1990**, *137*, 845–848.

(39) Hwang, J. T.; Chung, J. S. *Electrochim. Acta* **1993**, *38*, 2715–2723.

(40) Takasu, Y.; Ohashi, N.; Zhang, X.-G.; Murakami, Y.; Minagawa, H.; Sato, S.; Yahikozawa, K. *Electrochim. Acta* **1996**, *41*, 2595–2600.

(41) Mayrhofer, K. J. J.; Bliznac, B. B.; Arenz, M.; Stamenkovic, V. R.; Ross, P. N.; Markovic, N. M. *J. Phys. Chem. B* **2005**, *109*, 14433–14440.

(42) Kabbabi, A.; Gloaguen, F.; Andolfatto, F.; Durand, R. *J. Electroanal. Chem.* **1994**, *373*, 251–254.

(43) Bett, J.; Lundquist, J.; Washington, E.; Stonehart, P. *Electrochim. Acta* **1973**, *18*, 343–348.

(44) Watanabe, M.; Saegusa, S.; Stonehart, P. *Chem. Lett.* **1988**, 1487–1490.

(45) Watanabe, M.; Sei, H.; Stonehart, P. *J. Electroanal. Chem.* **1989**, *261*, 375–387.

(46) Yano, H.; Inukai, J.; Uchida, H.; Watanabe, M.; Babu, P. K.; Kobayashi, T.; Chung, J. H.; Oldfield, E.; Wieckowski, A. *Phys. Chem. Chem. Phys.* **2006**, *8*, 4932–4939.

Experimental Section

Chemicals. Sixth-generation poly(amidoamine) (PAMAM) dendrimers terminated with hydroxyl groups (G6-OH) were purchased as an 11.46% (w/w) solution in methanol (Dendritech, Inc., Midland, MI). Prior to use, the methanol was removed under vacuum. K_2PtCl_4 (99.99%), $NaBH_4$ (99.99%), and $LiClO_4$ (99.99%) were purchased from Sigma-Aldrich, Inc., and $HClO_4$ (Ultrex II) was from J. T. Baker. These reagents were used without further purification. Milli-Q deionized water (18 $M\Omega \cdot cm$, Millipore) was used to prepare aqueous solutions. Research-grade O_2 gas (Praxair, 99.999%) was used for the ORR experiments. N_2 gas (Praxair, 99.999%) and CO gas (Praxair, 99.9%) were also used.

Preparation of Pt DENs. Pt DENs were prepared by a previously reported procedure.^{5,8,9} Briefly, a 100 μM aqueous solution of G6-OH dendrimer and a 50 mM aqueous solution of K_2PtCl_4 were added to water in a vial. The final concentration of the G6-OH dendrimer was always 10 μM and the final concentration of K_2PtCl_4 ranged from 0.55 to 2.4 mM to achieve metal:dendrimer ratios of 55:1, 100:1, 147:1, 200:1, and 240:1. These solutions were stirred for 3 days to ensure Pt^{2+} binding to intradendrimer tertiary amines, and then a stoichiometric excess of freshly prepared, aqueous 1.0 M $NaBH_4$ was added to reduce Pt^{2+} . The final concentration of $NaBH_4$ was 20 mM. After addition of $NaBH_4$, the solutions were kept in sealed vials for 24 h to maximize reduction of Pt^{2+} .⁴⁷ Finally, the solutions were dialyzed for 24 h using a cellulose dialysis sack having a molecular weight cutoff of 12 000 (Sigma-Aldrich, Inc.) to remove impurities.¹⁰ The DENs resulting from this procedure are denoted as G6-OH(Pt_{55}), G6-OH(Pt_{100}), G6-OH(Pt_{147}), G6-OH(Pt_{200}), and G6-OH(Pt_{240}), where the numerical subscript represents the original $PtCl_4^{2-}$:G6-OH ratio used for the synthesis and hence the average number of Pt atoms in each DEN.

Characterization. UV–vis absorption spectra were obtained using a Hewlett-Packard HP8453 UV–vis spectrometer. The optical path length was 0.1 cm, and aqueous dendrimer solutions were used as references. TEM measurements were performed using a JEOL-2010F TEM. Samples were prepared by placing several drops of solution on a carbon-coated Cu TEM grid and allowing the solvent to evaporate in air.

Electrochemistry. Glassy carbon and Pt rotating disk electrodes (Pine Instruments, 5.0 mm diameter) were used for electrochemical experiments. The electrodes were prepared by successive polishing with 1.0 and 0.3 μm alumina powder on a polishing cloth (Buehler) followed by sonication in water for 5 min. The electrodes were then rinsed with water and dried under flowing N_2 gas. All electrochemical experiments were performed in a single-compartment, glass cell using a standard three-electrode configuration with a Pt-gauze (for Pt DEN immobilization) or an Au coil (ORR, H-adsorption/desorption, and CO stripping experiments) counter electrode and a mercury/mercurous sulfate reference electrode (CH Instruments, Inc., Austin, TX). For convenience, measured potentials are always converted to the potential of the reversible hydrogen electrode (RHE). Cyclic voltammetry and rotating disk voltammetry were performed using a computer-controlled Pine Instruments (Grove City, PA) AFRDE4 potentiostat and ASR rotator. All electrochemical experiments were performed at 22 ± 1 °C.

Results and Discussion

Characterization of Pt DENs. We have previously utilized the dendrimer templating method to prepare DENs having different sizes.^{1–4} Here, five different G6-OH(Pt_n) ($n = 55, 100, 147, 200, 240$) DENs were prepared and characterized by UV–vis spectroscopy and TEM. Figure 1a shows UV–vis absorption spectra of 10 μM G6-OH dendrimer containing K_2PtCl_4 with metal:dendrimer ratios of 55:1, 100:1, 147:1, 200:1, and 240:1 [$G6-OH(Pt^{2+})_n$] after stirring for 3 days. The spectra are comparable to our previous results.^{5,6,47–49} The absorbances at

(47) Knecht, M. R.; Weir, M. G.; Pyrz, W. D.; Ye, H.; Petkov, V.; Buttrey, D. J.; Frenkel, A. I.; Crooks, R. M. Manuscript in preparation.

(48) Ye, H.; Scott, R. W. J.; Crooks, R. M. *Langmuir* **2004**, *20*, 2915–2920.

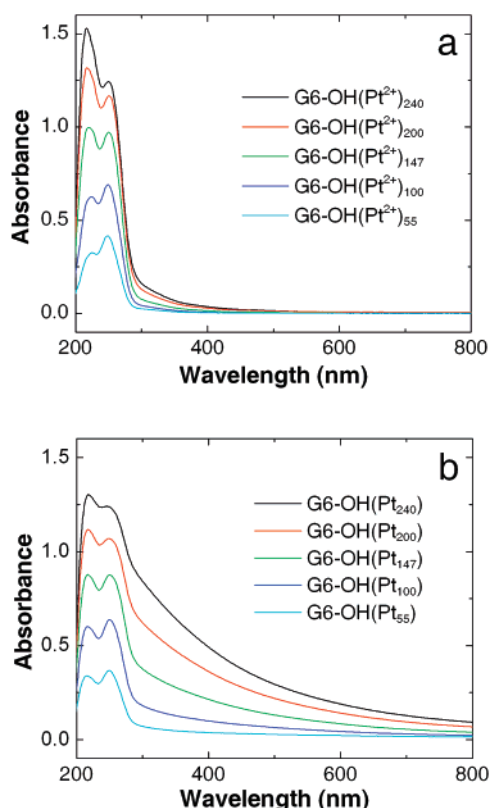


Figure 1. UV-vis absorption spectra of G6-OH(Pt²⁺)_n (*n* = 240, 200, 147, 100, and 55) (a) before and (b) after reduction. The final concentration of G6-OH(Pt²⁺)_n was 10 μM. The optical path length of the cell was 0.1 cm.

Table 1. Measured and Calculated Particle Sizes for Pt DENs

sample	av particle size, nm	calcd size, ^a nm	sample	av particle size, nm	calcd size, ^a nm
G6-OH(Pt ₂₄₀)	1.90 ± 0.29	1.91	G6-OH(Pt ₁₀₀)	1.52 ± 0.27	1.42
G6-OH(Pt ₂₀₀)	1.79 ± 0.26	1.79	G6-OH(Pt ₅₅)	1.44 ± 0.26	1.17
G6-OH(Pt ₁₄₇)	1.66 ± 0.25	1.62			

^a Calculated using the equation $n = 4r^3/3V_g$, where *n* is the number of Pt atoms, *r* is radius of the Pt nanoparticle, and *V_g* is the volume of one Pt (15.1 Å³) atom calculated from the molar volume.⁶⁷

220 and 250 nm arise from ligand to metal charge transfer bands associated with the Pt ions bound to internal tertiary amines of G6-OH. Figure 1b shows UV-vis absorption spectra of the same solutions after reduction with NaBH₄. These spectra reveal higher absorbances at longer wavelengths, which is characteristic of zerovalent metal particles having nanoscopic dimensions. Note, however, that the spectrum of the smallest DEN, G6-OH(Pt₅₅), does not change much after reduction compared to those having higher metal:dendrimer ratios. This is partially a consequence of its small size but may also indicate that lower metal ion:dendrimer ratios lead to stronger binding within the dendrimer and hence to higher reduction potentials.⁴⁷

Table 1 shows the average diameters and size distributions for the five DENs as well as their calculated diameters assuming a spherical geometry (TEM micrographs and histograms are provided in the Supporting Information, Figure S1). The particle sizes measured by TEM are generally close to the calculated sizes, except for G6-OH(Pt₅₅) and G6-OH(Pt₁₀₀). The higher-than-expected measured values for these DENs probably arise

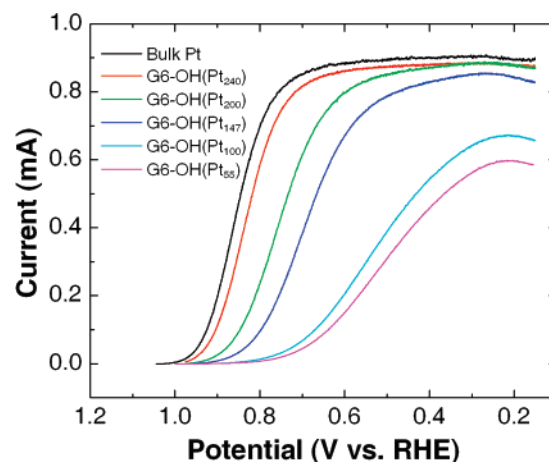


Figure 2. Rotating disk voltammograms (RDVs) for G6-OH(Pt_n)-modified GCEs (*n* = 240, 200, 147, 100, and 55) and for a bulk Pt electrode. The rotation rate was 900 rpm, the scan rate was 5 mV/s, and the geometric areas of GCE and bulk Pt electrodes were 0.196 cm². The electrolyte solution consisted of aqueous 0.1 M HClO₄ saturated with O₂.

from the difficulty of accurately counting very small particles.⁴ Regardless of this, the TEM results confirm that the five Pt DENs have sizes that generally reflect the synthesis conditions and that the size distributions are rather narrow. Hence, these materials are well-suited for studying the effect of particle size on the kinetics of the ORR.

Immobilization of Pt DENs on Glassy Carbon Electrodes (GCEs). The immobilization of Pt DENs on GCEs was performed using a previously reported procedure.^{8,9} Briefly, a freshly cleaned GCE was placed into 10 μM Pt DEN solution containing 0.1 M LiClO₄, and then the electrode potential was swept three times between 0.5 and 1.4 V (vs RHE). The resulting electrode was rinsed with water, sonicated in water for 5 min, and then used for electrochemical measurements. We have previously shown that this treatment provides robust attachment of DENs to GCEs and that the DENs are in good electrochemical communication with the electrode.⁸ We have also demonstrated that the nanoparticles are retained within the dendrimers following electrode immobilization.⁸

Rotating Disk Voltammetry. The ORR activity of Pt DENs was quantitatively measured using rotating disk voltammetry.⁹ The GCEs were modified with five different sizes of Pt DENs [G6-OH(Pt_n), *n* = 240, 200, 147, 100, 55], as described in the previous section, and the ORR kinetics of these materials were compared to that of a naked Pt rotating disk electrode (RDE). Figure 2 shows a series of rotating disk voltammograms (RDVs) for GCEs modified with the G6-OH(Pt_n) DENs and for the naked Pt RDE. The RDVs were obtained in O₂-saturated, aqueous 0.1 M HClO₄ using a rotation rate of 900 rpm and scanning the electrode potentials from 0.15 to 1.05 V (vs RHE) at a rate of 5 mV/s. Before measuring the RDVs shown in Figure 2, the DEN-modified electrodes were scanned 20 times at 100 mV/s between 1.0 and 0 V in the O₂-saturated, 0.1 M HClO₄ electrolyte solution. These preliminary scans are required to achieve stable and reproducible RDVs.

The RDV obtained using the bulk Pt electrode yields the highest ORR activity. The onset of catalytic current begins at about 1.0 V, and steady-state, mass-transfer-limited current is apparent over the range of 0.15 to 0.7 V. The RDV of the G6-OH(Pt₂₄₀)-modified GCE is shifted slightly negative compared to bulk Pt, but it has the same general shape. As the size of DENs is reduced further, the RDVs shift toward more positive potentials, indicating

Table 2. Summary of Kinetic Currents (i_K) and Specific Activities (SAs) for Bulk Pt and Pt DENs Measured at 0.80 and 0.85 V^a

catalyst	at 0.80 V			at 0.85 V		
	i_K (mA)	SA (mA/cm ²)		i_K (mA)	SA (mA/cm ²)	
		from CO	from H-des		from CO	from H-des
bulk Pt	2.94	9.44	9.37	0.97	3.10	3.07
G6-OH(Pt ₂₄₀)	1.67	1.95	2.78	0.51	0.59	0.85
G6-OH(Pt ₂₀₀)	0.31	0.65	0.97	0.10	0.21	0.32
G6-OH(Pt ₁₄₇)	0.10	0.45	0.70	0.03	0.14	0.23
G6-OH(Pt ₁₀₀)	0.013	0.20	0.37	-	-	-
G6-OH(Pt ₅₅)	0.007	0.21	0.45	-	-	-

^a i_K values for G6-OH(Pt₁₀₀) and G6-OH(Pt₅₅) were not obtained at 0.85 V, because no measurable ORR current was detected (Figure 2). Surface areas were calculated from CO oxidation (CO) or from H-desorption (H-des) measurements (see the text for details).

lower ORR activity. Additionally, the limiting current for the two smallest DENs is noticeably lower than for bulk Pt and the larger DENs; this observation is discussed later.

To obtain quantitative rates for the ORR as a function of particle size, the kinetic current for each Pt catalyst was calculated using the Koutecky–Levich equation (eq 1).^{9,50}

$$\frac{1}{i} = \frac{1}{i_K} + \frac{1}{i_d} = \frac{1}{i_K} + \frac{1}{0.20nFAD_0^{2/3}\omega^{1/2}\nu^{-1/6}C_0} \quad (1)$$

Here, i is the measured current, i_K is the kinetic current, i_d is the diffusion (mass-transfer) limited current, F is the Faraday constant, A is the geometrical electrode area (0.196 cm²), D_0 is the diffusion coefficient of O₂ (2.0 × 10⁻⁵ cm²/s),⁵¹ ω is the electrode rotation rate in units of rpm (900 rpm), ν is the kinematic viscosity of water (1.0 × 10⁻² cm²/s), and C_0 is the solubility of O₂ in dilute aqueous electrolyte solution (1.2 × 10⁻⁶ mol/cm³).^{51,52} Using the literature values provided above for the constants in eq 1, and $n = 4$ for the reduction of O₂ to H₂O, the calculated value of i_d is 0.87 mA. This is in good agreement with i_d values obtained from RDVs for bulk Pt, G6-OH(Pt₂₄₀), G6-OH(Pt₂₀₀), and G6-OH(Pt₁₄₇) (Figure 2). The RDVs for G6-OH(Pt₁₀₀) and G6-OH(Pt₅₅) exhibit low i_d values compared to the calculated values. Although we do not have a definitive explanation for this observation, it is possible that H₂O₂ becomes a significant product of the ORR for these very small catalytic particles. That is, i_d is predicted to range from 50% to 100% of the value obtained for conversion of oxygen to water (~0.87 mA, $n = 4$) when peroxide ($n = 2$) is a coproduct of the reaction. The i_K values at 0.80 and 0.85 V were calculated from the i and i_d values of the RDVs using eq 1. The resulting values of i_K (Table 2) are a representation of the ORR activity for each DEN catalyst. Consistent with previous results for particles having larger sizes,^{30,39–42} we find that i_K for the Pt-catalyzed ORR decreases monotonically as the particle size decreases.

Measurement of Pt DEN Surface Area. To accurately compare the activity of the DEN-modified electrodes discussed in the previous section, it is necessary to normalize i_K to the measured surface area of the Pt DENs. There are two accepted methods for determining the surface area of Pt catalysts: CO

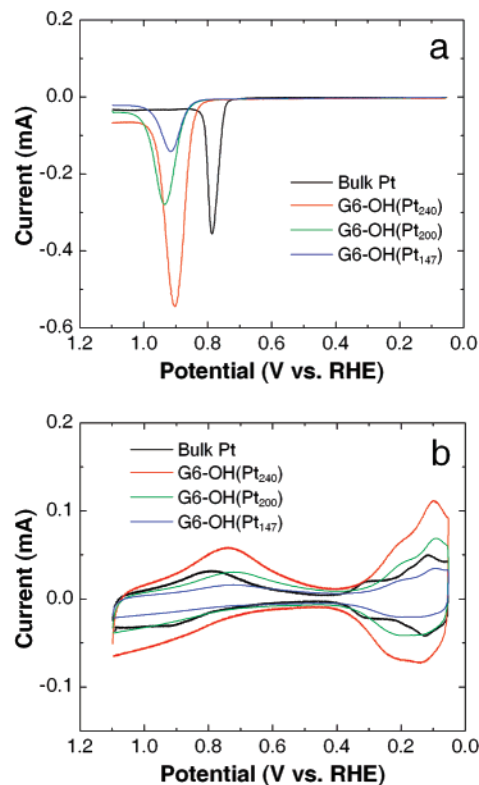


Figure 3. Cyclic voltammograms for G6-OH(Pt_{*n*})-modified GCEs ($n = 240, 200,$ and 147) and a bulk Pt electrode showing (a) CO oxidation and (b) H-adsorption/desorption. For each CV, the electrode potential was scanned from 0.05 to 1.1 V, back to 0.05 V, and then to 1.1 V again at a rate of 100 mV/s. For clarity, each CV was divided into the two parts shown in parts a and b. The electrolyte solution consisted of aqueous 0.1 M HClO₄ saturated with N₂. The electrode preparation is described in the corresponding section of the text. The geometric areas of GCE and bulk Pt electrodes was 0.196 cm².

stripping^{53–55} and H-adsorption/desorption.⁵⁶ We used both of these to measure the surface area of the Pt DENs and the bulk Pt electrode after obtaining the RDVs shown in Figure 2.

To estimate the surface areas, the electrodes were placed in a CO-saturated, 0.1 M HClO₄ solution, and the electrode potential was held at 0.05 V (vs RHE) for 10 min. This procedure results in strong adsorption of a monolayer of CO on the Pt surface.^{53–55} Next, without changing the electrode potential, the electrolyte solution was purged with N₂ gas for 15 min to remove CO gas from the solution. Finally, the electrode potential was scanned from 0.05 to 1.1 V, back to 0.05 V, and then to 1.1 V again at a rate of 100 mV/s. The resulting cyclic voltammograms (CVs) obtained from a bulk Pt electrode and from GCEs modified with the three largest DENs are shown in Figure 3. The CVs for G6-OH(Pt₁₀₀) and G6-OH(Pt₅₅) are not shown, because the magnitudes of their CO-stripping peaks were just above background on the scale used in this figure. Nevertheless, it was possible to integrate the peaks for these smaller DENs and obtain rough estimates of their surface areas.

During the first scan from 0.05 to 1.1 V (Figure 3a), oxidation peaks appeared at 0.79 V for bulk Pt and at 0.90–0.93 V for the Pt DENs. These peaks correspond to the oxidation of adsorbed

(50) Bard, A. J.; Faulkner, L. R. *Electrochemical Methods Fundamentals and Application*, 2nd ed.; John Wiley & Sons: New York, 2001; pp 340–344.

(51) *CRC Handbook of Chemistry and Physics, Internet Version 2007*; Lide, D. R., Ed.; Taylor and Francis: Boca Raton, FL, 2007; http://www.hbcpnet-base.com.

(52) Gubbins, K. E.; Walker, R. D., Jr. *J. Electrochem. Soc.* **1965**, *112*, 469–471.

(53) Gilman, S. J. *Phys. Chem.* **1962**, *66*, 2657–2664.

(54) Maillard, F.; Eikerling, M.; Cherstouk, O. V.; Schreier, S.; Savinova, E.; Stimming, U. *Faraday Discuss.* **2004**, *125*, 357–377.

(55) Maillard, F.; Schreier, S.; Hanzlik, M.; Savinova, E. R.; Weinkauff, S.; Stimming, U. *Phys. Chem. Chem. Phys.* **2005**, *7*, 385–393.

(56) Biegler, T.; Rand, D. A. J.; Woods, R. *J. Electroanal. Chem.* **1971**, *29*, 269–277.

Table 3. Measurements of Charge and Pt Surface Areas for a Bulk, Polycrystalline Pt Electrode and GCEs Modified with Pt DENs

catalyst	charge (μC)		area (cm^2) ^b			
	from CO	from H-des	from CO	from H-des	ratio of Pt areas (H/CO)	calcd area (cm^2)
bulk Pt	131	66	0.31	0.31	1.0	0.196 ^c
G6-OH(Pt ₂₄₀)	360	126	0.86	0.60	0.70	0.15
G6-OH(Pt ₂₀₀)	199	67	0.47	0.32	0.67	0.14
G6-OH(Pt ₁₄₇)	97	31	0.23	0.15	0.64	0.11
G6-OH(Pt ₁₀₀) ^a	27	7.5	0.064	0.036	0.56	0.085
G6-OH(Pt ₅₅) ^a	14	3.2	0.033	0.015	0.46	0.058

^a These results are not as reliable as the others because the CO oxidation and H-desorption peaks were only slightly above the background level.

^b Surface areas were calculated from CO oxidation (CO) or from H-desorption (H-des) measurements (see the text for details). ^c The calculated area for the bulk Pt RDE is its geometric area and does not include a roughness factor.

CO. The absence of this peak in the second scan (Figure 3b) confirms that CO oxidation arises primarily from adlayers and not from dissolved CO. Compared to the bulk Pt electrode, the CO oxidation peak was shifted 110–140 mV positive. This shift is consistent with the more coordinatively unsaturated atoms on the surface of smaller particles and hence stronger CO adsorption compared to bulk Pt. Note that while the CO oxidation peaks for the nanoparticles were always shifted positive compared to bulk Pt, there was enough run-to-run variability in the peak position (typically ± 15 mV) that it is not possible to correlate the magnitude of this shift to particle size. However, there have been reports in the literature relating shifts in CO oxidation peaks to particle size,^{41,54,55,57} and still others in which no size-dependent shifts were observed for Pt nanoparticles in the 1–5 nm size range.^{58,59}

Integration of the CO oxidation peaks makes it possible to estimate the total Pt surface area. Note, however, that this calculation requires information about the amount of charge required to oxidize CO per unit area of Pt. The accepted value for this constant is $420 \mu\text{C}/\text{cm}^2$,^{53–55} but this value was determined using bulk-phase, polycrystalline Pt.⁵³ To the best of our knowledge there are no corresponding data for Pt nanoparticles, and therefore, we wish to emphasize that surface areas determined using this value must be viewed with caution. The total charge passed to oxidize CO and the corresponding surface areas for bulk Pt and the five DEN-modified electrodes are given in Table 3. We will return to the significance of these values shortly.

We also estimated the Pt surface areas using the hydrogen-desorption peaks in the range 0.05 and 0.3 V (Figure 3b).^{56,60} However, this method for evaluating surface areas suffers from the same problem as the CO-oxidation approach: while there are reliable values for the charge-per-area required to desorb hydrogen on well-defined, planar surfaces, such values are not available for nanoparticles. The accepted literature value for the charge density for Pt(111) and the average for the three low-index planes (100), (110), and (111) of Pt is $210 \mu\text{C}/\text{cm}^2$.^{56,60} The charge densities and estimated surface areas determined for DENs and bulk Pt by the hydrogen desorption method are also summarized in Table 3.

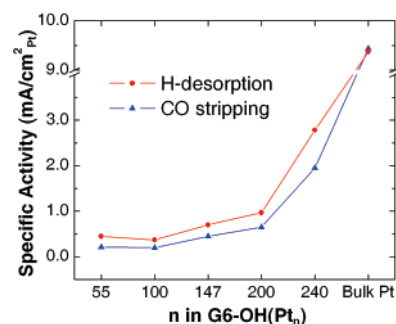


Figure 4. Comparison of specific activities (at 0.80 V) for a bulk polycrystalline electrode and GCEs modified with Pt DENs [G6-OH(Pt_n), $n = 240, 200, 147, 100,$ and 55]. The specific activities were calculated by normalizing i_K to the total Pt surface areas measured by either CO oxidation (blue triangles) or H-desorption (red circles).

Both methods for determining the surface area reveal the same qualitative trend: the total Pt surface area decreases as the sizes of the DENs decreases. However, the surface areas obtained by the CO oxidation method are higher than those obtained by H-desorption, and this effect is most pronounced for the smallest particles. A similar trend has been observed for Pt nanoparticles having diameters of < 2 nm in previous studies.^{54,61}

By making a few reasonable assumptions, it is possible to calculate the surface area of the Pt DENs for comparison to the experimentally determined values.⁹ We have previously shown that dendrimers form near-monolayer coverages on most surfaces.⁶² Therefore, by assuming monolayer dendrimer coverage, a projected area for each dendrimer of 35 nm^2 ,⁹ that one nanoparticle is encapsulated within each dendrimer, that each nanoparticle is spherical, and that the roughness factor of GC surfaces is 2.4, which is an average value from the literature (range 1.3–3.5),^{63–65} the calculated surface areas shown in Table 3 can be derived. The calculated areas are smaller than the measured areas for the G6-OH(Pt₂₄₀), G6-OH(Pt₂₀₀), and G6-OH(Pt₁₄₇) DENs and larger than the measured areas for the G6-OH(Pt₁₀₀) and G6-OH(Pt₅₅) DENs. Clearly, the discrepancy between the measured and calculated values arises because one or more of the assumptions that goes into the calculation is incorrect. The assumption most likely to dominate the discrepancies are the charge-density values ($420 \mu\text{C}/\text{cm}^2$ for CO stripping and $210 \mu\text{C}/\text{cm}^2$ for H-desorption), which, as mentioned earlier, are just estimates based on bulk Pt.

The specific activities (SAs) for the five DENs are determined by dividing the kinetic currents (i_K) by the experimentally determined surface areas. This is an important step, because it provides a direct comparison of the kinetic properties of DENs having different sizes. Table 2 shows the SAs for bulk Pt and for the DENs at 0.80 and 0.85 V based on the surface areas determined by both CO oxidation and H-desorption. Figure 4 compares the SA values determined at 0.80 V graphically. Bulk Pt exhibits the highest SA value ($9.4 \text{ mA}/\text{cm}^2 \text{ Pt}$ at 0.80 V). The Pt DENs exhibit much lower SA values, and there is a clear monotonic decrease in SA as the particle size decreases. Because the dendrimers are the same for all the DENs and because the number of dendrimers (and hence the number of DENs) should

(57) Cherstiouk, O. V.; Simonov, P. A.; Savinova, E. R. *Electrochim. Acta* **2003**, *48*, 3851–3860.

(58) Arenz, M.; Mayrhofer, K. J. J.; Stamenkovic, V.; Blizanac, B. B.; Tomoyuki, T.; Ross, P. N.; Markovic, N. M. *J. Am. Chem. Soc.* **2005**, *127*, 6819–6829.

(59) Mayrhofer, K. J. J.; Arenz, M.; Blizanac, B. B.; Stamenkovic, V.; Ross, P. N.; Markovic, N. M. *Electrochim. Acta* **2005**, *50*, 5144–5154.

(60) Pozio, A.; De Francesco, M.; Cemmi, A.; Cardellini, F.; Giorgi, L. J. *Power Sources* **2002**, *105*, 13–19.

(61) Friedrich, K. A.; Henglein, F.; Stimming, U.; Unkauf, W. *Electrochim. Acta* **2000**, *45*, 3283–3293.

(62) Tokuhisa, H.; Zhao, M.; Baker, L. A.; Phan, V. T.; Dermody, D. L.; Garcia, M. E.; Peez, R. F.; Crooks, R. M.; Mayer, T. M. *J. Am. Chem. Soc.* **1998**, *120*, 4492–4501.

(63) Lee, C.-W.; Bard, A. J. *J. Electroanal. Chem.* **1988**, *239*, 441–446.

(64) Pontikos, N. M.; McCreery, R. L. *J. Electroanal. Chem.* **1992**, *324*, 229–242.

(65) Rice, R. J.; McCreery, R. L. *Anal. Chem.* **1988**, *61*, 1637–1641.

be the same,⁶² we conclude that these results establish a relationship between catalyst size (in the 1–2 nm size range) and activity. At present, we are working toward establishing a first-principles understanding of this relationship, but this will require detailed calculations and a better understanding of the structure of the nanoparticles.

It is possible to compare the ORR activity of Pt DENs to commercial carbon-supported Pt (Pt/C) catalysts. The SAs of Pt/C (ETEK or TKK) ranges from 0.19 to 0.23 mA/cm² Pt at 0.9 V under conditions similar to those used here (except for the temperature, which was 60 °C). The surface areas for the Pt/C catalysts were determined using hydrogen adsorption/desorption.³⁰ We calculated the SA value for G6-OH(Pt₂₄₀) at 0.9 V using the same method used to derive the values in Table 2. These SA values were 0.15 mA/cm² Pt (surface area based on CO oxidation) and 0.21 mA/cm² Pt (surface area based on H-desorption), which are comparable to the SA values reported for commercial Pt/C catalysts.³⁰

Summary and Conclusions

We have examined the effect of catalyst sizes on the electrochemical ORR. The most important conclusion reported here is that nearly monodisperse Pt nanoparticles having well-defined sizes in the 1–2 nm range can be prepared by the dendrimer templating method and that differences in the sizes of these materials produce clearly distinguishable effects on the ORR kinetics. The clear trend is that smaller particles exhibit lower specific activities. Indeed, two sets of catalysts varying in average size by only 40 Pt atoms [G6-OH(Pt₂₄₀) and G6-OH(Pt₂₀₀)] exhibit easily distinguishable activities.

The dendrimer templating method offers an excellent opportunity to better understand the effect of catalyst size on chemical and electrochemical reactions. For example, we previously showed a similar effect of catalyst size on a homogeneous hydrogenation reaction.² The key attributes of the method are that it provides a high degree of control over catalyst size and monodispersity. Moreover, because the dendrimer template is porous, it can be retained during catalytic measurements, and this probably reduces or eliminates agglomeration of the catalysts during operation. The dendrimer also provides a means for robust anchoring of the catalyst to surfaces. Of course, there are some additional aspects of the DEN configuration that

are as yet not fully understood. For example, the dendrimer itself may influence kinetic measurements. Although EXAFS measurements have shown that most of the DEN surface is not interacting with the dendrimer to a measurable degree,⁶⁶ it is likely that the activity of the DEN is modulated to some extent by either mass-transfer inhibition (that is, reduced transport rate of substrate through the dendrimer prior to its arrival at the catalyst surface) or direct kinetic inhibition (for example, blocked surface sites or changes to the electronic and geometric properties of the nanoparticle). These are issues that we are just beginning to address, but the small size of DENs presents some unique analytical challenges that must be overcome before conclusive results can be reported.

Finally, a central objective of contemporary catalysis research is to construct experimental models that can be directly compared to theory, and we believe DENs will provide one means to address this goal. Accordingly, we are also beginning to apply first-principle calculations to both mono- and multimetallic catalysts of the type described here. Reports of progress in these areas will follow in due course.

Acknowledgment. We gratefully acknowledge the U.S. Department of Energy, DOE-BES Catalysis Science Grant No. DE-FG02-03ER15471, the Robert A. Welch Foundation, and the National Science Foundation (Grant No. 0531030) for financial support of this project. We also acknowledge SPRING and the Robert A. Welch Foundation for support of some of the instrumentation used in this project. We thank Dr. Ji-Ping Zhou of the Texas Materials Institute at UT–Austin for help with the TEM measurements. We are especially grateful to Prof. Carol Korzeniewski (Texas Tech University) and Prof. Daniel A. Scherson (Case Western Reserve University) for enlightening discussions.

Supporting Information Available: TEM images and particle-size distributions for G6-OH(Pt_n) (*n* = 55, 100, 147, 200, 240) DENs. This material is available free of charge via the Internet at <http://pubs.acs.org>.

LA702297M

(66) Knecht, M. R.; Weir, M. G.; Frenkel, A. I.; Crooks, R. M. *Chem. Mater.* In press.

(67) Leff, D. V.; Ohara, P. C.; Heath, J. R.; Gelbart, W. M. *J. Phys. Chem.* **1995**, *99*, 7036–7041.